CFD Simulation of the Fluid Hydrodynamics in a Continuous Stirred-Tank Reactor

Shuo Zhang*, David Müller, Harvey Arellano-Garcia, Günter Wozny

Chair of Process Dynamics and Operation, Berlin Institute of Technology, Sekr. KWT-9, Str. des 17. Juni 135, D-10623 Berlin, Germany
shuo.zhang@campus.tu-berlin.de

Continuous stirred-tank reactors (CSTR) are widely applied in the chemical, food, and pharmaceutical engineering fields. The micro-scale fluid dynamics are important for the optimal processing study since they have a dominating influence on the overall performance of the reactor. In this article, 3-dimensional Computational Fluid Dynamics (CFD) simulations are carried out to portray the flow characters in the CSTR of the mini-plant of the Collaborative Research Center InPROMPT coordinated by the Technische Universität Berlin. In InPROMPT, the reactor is used to perform a rhodium-catalyzed hydroformylation of long chain alkenes. In this study, cases of a vessel with and without baffles are compared. The results show the existence of a high speed velocity toroidal zone in different horizontal sections in the CSTR without baffles, comparing to the common pervasive conception which is the assumption of a complete uniformity of the fluid velocity magnitude in a CSTR at the final steady state. Moreover, under the rotation speed of 400 rpm, the baffles in the CSTR can significantly prevent the formation of a surface vortex, for the mean tangential velocity magnitude is dramatically decreased. On the other hand, the mean radial and axial velocity is tremendously increased when the baffles are added. Therefore, the baffles in the tank lead to a greater vertical fluid exchange in CSTR. Besides, in the specific domain of CSTR region, both the fluid velocity direction and magnitude carry on a cyclical variation, when the baffles are inserted into the CSTR.

1. Introduction

Continuous stirred-tank reactors (CSTR) are widely applied in the chemical, food, and pharmaceutical engineering fields, for their good mixing ability and scale-up characteristics (Liu et al., 1997). At Berlin University of Technology (Technische Universität Berlin), Germany, a novel process concept for the hydroformylation of long chain alkenes in micro emulsions is currently being developed in the Collaborative Research Centre SFB/TR 63 InPROMPT, "Integrated chemical processes in liquid multiphase systems". In this project, a homogenous catalysis hydroformylation chemical reaction is to be performed in a continuous stirred-tank reactor (Müller et al., 2013).
Under turbulent (high Reynolds number) conditions, the mixing efficiency can be enhanced by using rectangular boards (called Baffles). Generally, baffles are symmetrically installed and mounted vertically in an agitated tank. Although it is known that the convective flow in a tank with baffles becomes more complex than in one without baffles (Sadhan et al., 1994), the detailed fluid dynamics is still unclear. The aim of this contribution is to capture and describe the structure of the convective flow in the CSTR, where the hydrodynamics of the CSTR with and without baffles are compared. With the help of the information gained through the CFD simulations, ideal operating parameters as well as equipment aspects for the CSTR are considered.

2. Methodology

The multi-phase flow in the CSTR in this study consists of two phases: a dispersed phase (gas) in the top and a continuous phase (liquid) in the bottom. In computational fluid mechanics, there are currently two approaches for numerical calculation of multiphase dynamics: the Euler-Lagrange and the Euler-Euler

approach. In the first, the fluid phase is treated as a continuum by solving the Navier-Stokes equations, while the dispersed phase is solved by tracking a large number of particles through the calculated flow field. The dispersed phase can exchange momentum, mass, and energy with the fluid phase. This approach can track the trajectory of the disperse phase by introducing a Lagrangian grid, but with huge calculation load. The latter approach introduces the concept of a phasic volume fraction (PVF), which is assumed to be continuous functions of space and time in the computational mesh domain. The fixed grid technology method is implemented in the Euler-Euler approach which allows the reduction of memory space consummation and computational cost. However, with appropriate discretization schemes, these two approaches show no substantial differences (Sokolichin et al., 1997). As a result, the Euler–Euler approach is preferred for a majority of multi-phase simulations. In the Euler-Euler approach, the Volume of fluid (VOF) model is one of the most wildly used and important multi-phase models for the immiscible fluids where the position of the interface between the fluids is of interest. The VOF model mainly focuses on the capture and the track of the multi-phase interface.

One major part of the investigated CSTR is the agitated impeller. It generates the rotating flow domains in the reactor. In computational fluid dynamics, problems involving rotating flow domains usually have a stationary (or inertial) reference frame and a moving (or non-inertial) reference frame. In these cases, the moving parts are considered as an unsteady problem when viewed from the stationary frame. Nevertheless, in a moving reference frame, the flow around the moving parts can be modelled as a steady-state problem. It is advantageous to solve the equations with respect to the moving reference frame. Therefore, the moving reference frame (MRF) model is implemented to simulate the agitated impeller involving rotating blades in the CSTR.

2.1 The VOF Model

In the VOF model, a single set of momentum equations is employed by both the dispersed phase and the continuous phase, which means both phases share common pressure and velocity fields. The VOF model with a piecewise-linear geometric reconstruction scheme is chosen to trace the interface between the gas and liquid phase, which is based on the volume fraction of the liquid phase (primary phase) $\emptyset_L$. The equation is expressed as:

$$\frac{\partial}{\partial t}(\emptyset_L) + \nabla(\emptyset_L \vec{v}) = 0 \tag{1}$$

So as for the gas phase (secondary phase), the volume fraction $\emptyset_G$ is:

$$\emptyset_G + \emptyset_L = 1 \tag{2}$$

For the Newtonian fluid, the momentum conservation in the VOF model is the Navier-Stokes equation:

$$\frac{\partial}{\partial t}(\rho_m \vec{v}) + \nabla(\rho_m \vec{v}\vec{v}) = -\nabla p + \nabla[\mu_m(\nabla\vec{v} + \nabla\vec{v}^T)] + \vec{F_s} \tag{3}$$

Where ρ_m and μ_m are respectively the volume averaged mixture density and viscosity of gas and liquid phases as the following:

$$\rho_m = \emptyset_L \rho_L + (1 - \emptyset_L)\rho_G \tag{4}$$

$$\mu_m = \emptyset_L \mu_L + (1 - \emptyset_L)\mu_G \tag{5}$$

$\vec{F_s}$ is the momentum source force term, regarded as the external forces exert on the both phases such as the gravity and the surface tension:

$$\vec{F_s} = \vec{F_g} + \vec{F_\sigma} \tag{6}$$

For the gravity is a typical body force, the gravity source term expression is in the form below:

$$\vec{F_g} = \rho_m \vec{g} \tag{7}$$

Surface tension has the dimension of force per unit area. Referring to the Continuum Surface Force (CSF) proposed by Brackbill et al. (1992), the force at the surface can be expressed as a volume force using the divergence theory. The surface tension source term $\vec{F_\sigma}$ is converted from the surface force to a body force in the description of the following:

$$\vec{F_\sigma} = \sigma \frac{\rho_m \kappa \nabla \emptyset_L}{0.5(\rho_G + \rho_L)} \tag{8}$$

Where the curvature κ is defined in terms of the divergence of the unit normal $\hat{n}$:

$$\kappa = \nabla\hat{n} \qquad \hat{n} = \frac{n}{|n|} \tag{9}$$

$$\kappa = \frac{1}{|n|} [\left(\frac{n}{|n|}\nabla\right)|n| - (\nabla n)] \tag{10}$$

Where, the interfacial delta function $\nabla\emptyset_L$ is one in the surface domain and zero away from the surface domain which guarantees that the surface tension is only active in the region of an inter-phase surface.

2.2 The MFR Model

The MRF model is implemented to emulate the region involving agitated impeller. In the model, selected moving cell zones are activated as the moving reference frame, in which the momentum equations are modified including the additional acceleration terms. Additionally, the interface between the stationary and moving frame is treated as velocity and velocity gradient change with the adjacent cell zones. The scalar quantities such as temperature, pressure, density, turbulent kinetic energy, etc. stay unchanged.

A coordinate frame relative to a stationary (inertial) reference frame, which is translating with a linear velocity $\vec{v}_r$ and rotating with angular velocity, $\vec{\omega}_r$ is taken into consideration. The position vector between the moving reference frame and stationary reference frame is $\vec{d}_0$. The calculation domain is located at a position vector $\vec{d}_r$ with respect to the origin of the moving reference frame. $\vec{v}_m$ is the relative velocity (the velocity viewed from the moving frame), $\vec{v}_s$ is the absolute velocity (the velocity viewed from the stationary frame), $\vec{u}_r$ is the moving frame relative to the inertial frame. Their expressions are as follows:

$$\vec{v}_s = \vec{v}_m + \vec{u}_r \tag{11}$$

$$\vec{u}_r = \vec{v}_r + \vec{\omega}_r \times \vec{d}_r \tag{12}$$

Conservation of momentum in the MFR model is achieved with the Navier-Stokes equation:

$$\frac{\partial}{\partial t}(\rho\vec{v}_m) + \nabla \cdot (\rho\vec{v}_m\vec{v}_m) + \rho\left(2\vec{\omega}_r \times \vec{v}_m + \vec{\omega}_r \times \vec{\omega}_r \times \vec{d}_r + \vec{\alpha}_r \times \vec{d}_r + \vec{a}_t\right) = -\nabla p + \nabla \cdot \overline{\overline{\tau}}_r + \vec{F} \tag{13}$$

$$\vec{\alpha}_r = d\vec{\omega}_r/dt \text{ and } \vec{a}_t = d\vec{v}_t/dt \tag{14}$$

It contains four additional acceleration terms. The first two terms are the Coriolis acceleration $(2\vec{\omega}_r \times \vec{v}_m)$ and the centripetal acceleration $(\vec{\omega}_r \times \vec{\omega}_r \times \vec{d}_r)$ respectively. The third and the fourth are due to the acceleration of the rotational speed $(\vec{\alpha}_r \times \vec{d}_r)$ and translational velocity $(\vec{a}_t)$ respectively. In addition, $\overline{\overline{\tau}}_r$ is the stress tensor and μ is the molecular viscosity. I is the unit tensor, and $2/3\nabla \cdot \vec{v}_m I$ is the effect of volume dilation (Batchelor et al., 1967), defined as:

$$\overline{\overline{\tau}}_r = \mu[\left(\nabla\vec{v}_m + \nabla\vec{v}_m^T\right) - \frac{2}{3}\nabla \cdot \vec{v}_m I] \tag{15}$$

3. Simulation Description

The object of the study is based on a CSTR for a rhodium-catalyzed hydroformylation chemical process in InPROMPT project. The CSTR is a stirred cylindrical tank agitated by a single concentric Rushton impeller (6 blades, 45 mm in diameter, 10 mm in both length and width for each blade) located 50 mm above the bottom of the tank. The mix vessel is a glass tank with an inner diameter of 90 mm and a height of 160 mm. The initial water level is at a height of 140 mm. The comparison of the un-baffled and baffled case will be carried out at the rotational speed of 400 rpm. Four baffles with 150 mm length, 7 mm width and 2 mm thickness, are set 5 mm away from the CSTR wall. Figure 1, shows the detailed dimensions of the CSTR with baffles and without baffles.
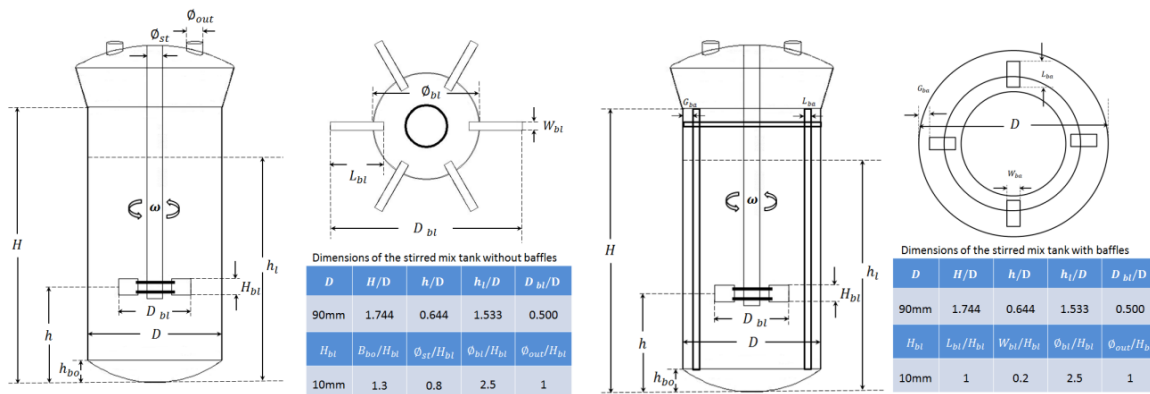

Dimensions of the stirred mix tank without baffles

D	H/D	h/D	h_l/D	D_{bl}/D
90mm	1.744	0.644	1.533	0.500

H_{bl}	B_{bo}/H_{bl}	$\emptyset_{st}$/H_{bl}	$\emptyset_{bl}$/H_{bl}	$\emptyset_{out}$/H_{bl}
10mm	1.3	0.8	2.5	1

Dimensions of the stirred mix tank with baffles

D	H/D	h/D	h_l/D	D_{bl}/D
90mm	1.744	0.644	1.533	0.500

H_{bl}	L_{bl}/H_{bl}	W_{bl}/H_{bl}	$\emptyset_{bl}$/H_{bl}	$\emptyset_{out}$/H_{bl}
10mm	1	0.2	2.5	1

Figure 1. Schematic diagram of the CSTR: Left (without baffle), Right (with baffle)

A careful selection of the mesh type and number is considered before the simulation. These have a significant influence for calculation accuracy and efficiency. In 90% of the overall volume of the CSTR hexahedron mesh type is used in the meshing scheme for its higher calculation accuracy in 3-dimension multi-phase simulation (Handbook of Ansys, 2012).In order to determine the mesh size considering both computational capacity and the result validity, different radial velocity magnitude profiles (z=90 mm, x axis positive) at 60s for different mesh sizes of 1mm, 2mm, 3mm, 5mm, and 7mm are compared in Figure 2 left. Based on the results, mesh size of 2mm is adequate to capture the feature flow in the CSTR and is used in the subsequent simulations. The original point of the reference coordinate is set to the center point of the bottom disk plane.
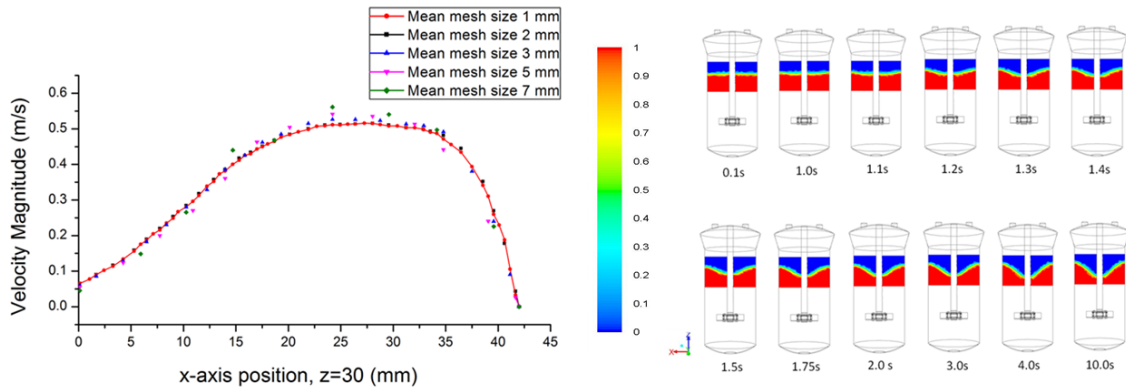

Figure 2. Radial profile of velocity magnitude (z=90 mm) corresponding to different mesh size at 60s (left). Contours of the volume fraction without baffles at 400 rpm (unit: m3/m3) (right).

Three-dimensional transient simulations are carried out with the commercial CFD software Ansys FLUENT 14.0 on a computer of the i7 (3.5GHz) Octal-core CPU and 16 GB memory in a parallel model. In the simulations, the average liquid velocity in the xy-plane (z=90 mm) is monitored. When there is no obvious change or a period change of the velocity value with different iterate time steps and all residuals are always in the coverage restriction, the simulation is terminated for achieving steady state. In additional, it is proven that there is a turbulent flow in the stirred tank system (Alopaeus, et al., 1999) as well as in the system with baffles. Therefore, the RNG k-ε Turbulence Model (Orszag, et al., 1993) is implemented in the simulations mentioned above. The operating conditions and the physical material properties in simulations are listed in Table 1.

Table 1: Operation conditions and Material properties

Parameter	Value	Unit
Temperature	288	K
Pressure	1.013×10^5	Pa
Gravity $(\vec{g})$	9.8	m/s^2
Liquid density (ρ_L)	998.2	kg/m^3
Gas density (ρ_G)	1.225	kg/m^3
Liquid viscosity (μ_L)	1.003×10^{-3}	kg/(m·s)
Gas viscosity (μ_G)	1.789×10^{-5}	kg/(m·s)
Surface tension (σ)	7.19×10^{-2}	N/m

4. Results and Discussion

4.1 Vortex formation

When the agitated impeller in CSTR starts rotating the liquid swirls around the tank, the centrifugal force appears and draws liquid away from the centre of rotation. The centrifugal force leads to formation of a vortex, see Figure 2 right. A comparison between simulations and experiments is displayed in Figure 3. The scale is the phase volume fraction with the unit mm3/mm3. The value 1 means 100% water, 0 means there is no water there, and 0.5 means the water level where there is half water and half air in volume at that location. The simulation result at a rotation speed of 400 rpm demonstrates that after almost 1s the fluid near the surface fluctuates. After 4s, the vortex is formed and the water surface is at steady state. At 10s, the vortex (phase volume fraction is 0.5) height from the top to the bottom is 31.64 mm. Both simulation and experiment have illustrated the existence of a vortex interface in CSTR at the speed of 400 rpm. The vortex height is 38.83 mm in the experiment (top to bottom). In order to eliminate the vortex, four baffles are inserted to the tank. With these, the vortex height is 2.3mm in simulation and 1.8mm in experiment respectively, a considerable decrease from the contrast case without baffles.
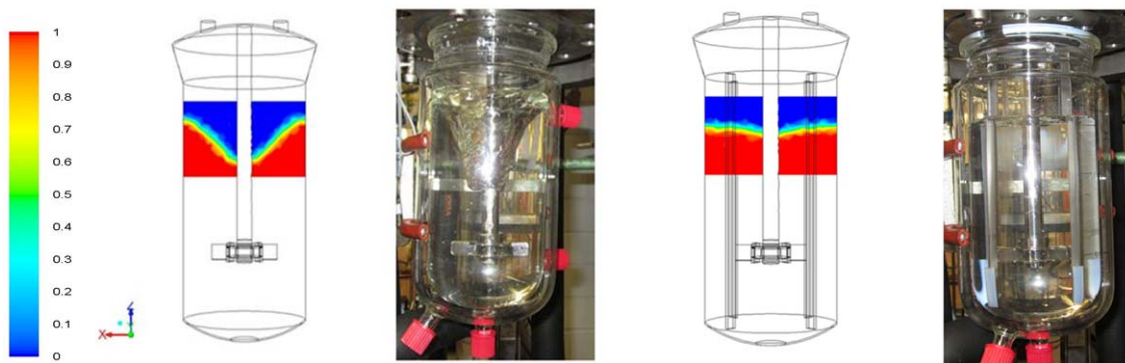
Figure 3. Vortex in the CSTR with and without baffles at 400 rpm simulation and experiment (unit: m^3/m^3).

4.2 Vertical sections of velocity contours

The velocity profile is an important parameter for describing the performance of the CSTR. Figure 4 shows the contours of the velocity magnitude on 7 typical xy-plane sections with the distance 10, 30, 50, 70, 90, 110, and 130 mm from the tank bottom. At the beginning, the fluid near the impeller follows the blades. Afterwards, the fluid extends up to the tank top and down towards tank bottom simultaneously. At 10s, the mean velocity in the tank without baffles is as follows: 0.453, 0.4484, 0.528, 0.4439, 0.4552, 0.4516, and 0.3941 m/s. The simulation result presents that the fluid velocity near the stirring rod in the tank center is much lower as that near the tank wall. There is a high speed toroidal zone in every section.

Figure 4 shows the contours of the velocity magnitude on 7 typical xy-plane sections with the distance 10, 30, 50, 70, 90, 110, and 130 mm from the tank bottom in a CSTR with baffles. At 10s, the mean velocity in the tank with baffles on these sections is as follows: 0.2023, 0.1713, 0.5351, 0.1939, 0.1659, 0.1324, and 0.1067 m/s, a notable decreasing compared to the velocities without baffles. The simulation result presents that the fluid velocity in the tank with baffles is much slower than that in the tank without baffles, despite the mean velocity of the section which is 50 mm away to the tank bottom (the section includes the impeller blades) stays at the same value (with baffles: 0.5351 m/s; without baffles: 0.5280 m/s).
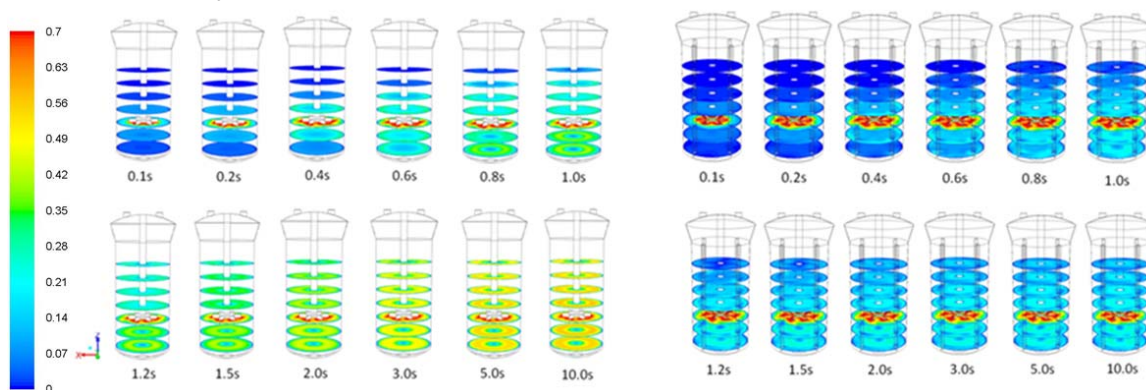

Figure 4. Contours of the velocity sections in CSTR with baffles and without baffles (unit: m/s)

4.3 Periodic velocity magnitude in a CSTR with baffles

There is an interesting finding in the case of the CSTR with baffles that the velocity magnitude carries a periodic variation in certain regions instead of a conventional assumption that the velocity magnitude is always a constant in steady state. Points I~III are in the same xy-plane with different radius (20 mm, 30 mm and 40 mm) to the centre below the impeller and point IV is located in the xy-plane above the impeller with the same radius as point II. Figure 5 shows the velocity variation at four typical points (I~IV) from 0 to 20s in the CSTR with and without baffles respectively. The simulation results illustrate that all the four points become constants after 5s at a rotational speed of 400 rpm at steady state in the CSTR without baffles. However, in the CSTR with baffles under the same rotational speed, all the four points enjoy a non-synchronous periodical change at steady state. The velocity magnitude period of the four points is approximately 6 seconds in common. Moreover, point IV, which is located in the xy-plane 40mm above the impeller, demonstrates smaller amplitude than the other three points that are situated in the xy-plane 20mm below the impeller. It is also worth mentioning that point I, located below the agitated blades, carries on a non-sinusoidal wave which implies that there is the co-effect of multi periodic flows with different frequency at that point.
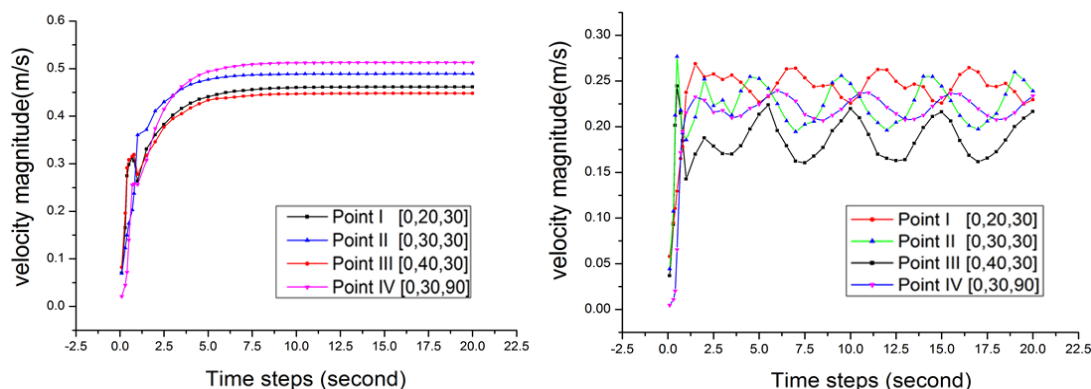
Figure 5. Velocity variation at four typical points in CSTR without (constant) and with baffles (periodic).

5. Conclusions and Outlook

In general, the hydrodynamics in a CSTR under rotational speed of 400 rpm is much more complicated than that in a laminar flow CSTR with a low Re number, especially, when baffles are introduced. From simulation and experiment the conclusion is made that baffles have a tremendous influence to eliminate the formation of a vortex. Baffles suppress the tangential velocity which prevents the vortex formation. Moreover, the baffles lead to an increase in the radial and axial velocity, so that the flow circulation is improved for enhanced mixing. Interestingly, in the CSTR with baffles, the velocity magnitude of certain regions carries a non-synchronous periodic variation for the non-total sectional symmetry baffles structure. The results show that a reactor with baffles is essential for efficient mixing. Furthermore, in contrast to general assumptions that faster rotating speeds lead to a better mixing of the system, the CFD-Simulations show that a too fast stirrer speed may, even in the presence of baffles, lead to the formation of a vortex.

This work concentrates on simulating a system consisting of water and air. In later simulations, the real system applied in InPROMPT will be investigated. All these results provide a fundamental contribution for the succeeding multi-phase dynamics investigation where the additional gas injection is added as well as the improvement for the gas holdup and bubble distribution in CSTR. The optimal stirrer speed will be determined, while considering gas injection, gas holdup, bubble size, and vortex formation.

Acknowledgments

References

Lu W. M., Wu H. Z., Ju M. Y. 1997，Effects of baffles design on the liquid mixing in an aerated stirred tank with standard Rushton turbine impellers, Chemical Engineering Sicence, 52, 3843-3851.

Müller M., Kasaka Y., Müller D., Schomäcker R., Wozny G., 2013, Process Design for the Separation of Three Liquid Phases for a Continuous Hydroformylation Process in a Miniplant Scale, Industrial Engineering Chemical Research, DOI: 10.1021/ie302487m.

Sandhan C.J., Tjahjadi M., Ottino J.M., 1994, Chaotic mixing of viscous fluid by periodic changes in geometry: baffled cavity flow, AIChE Journal, 40, 1769-1781.

Sokolichin A., Eigenberger G., Lapin A., Lubbert A., 1997, Dynamic Numerical Simulation of Gas-Liquid Two-Phase Flows Euler/Euler Versus Euler/Lagrange, Chemical Engineering Science, 52, 611–626.

Brackbill J. U., Kothe D. B., Zemach C., 1992, A Continuum Method for Modeling Surface Tension, Journal of Computational Physics, 100, 335–354.

Batchelor G. K. 1967, An Introduction to Fluid Dynamics, Cambridge Univ.Press, Cambridge, England.

Handbook of Ansys FLUENT 14.0, 2012, User's Guide, ANSYS, Inc. Pittsburgh, USA.

Alopaeus V., Koskinen J., Keskinen K.I., 1999, Simulation of the population balances for liquid–liquid systems in a nonideal stirred tank. Part 1—description and qualitative validation of the model, Chemical Engineering Science, 54, 5887-5899.

Orszag S. A., Yakhot V., Flannery W. S., Boysan F., Choudhury D., Maruzewski J., Patel, B., 1993, Renormalization Group Modeling and Turbulence Simulations, International Conference on Near-wall turbulent flows, So R.M., Speziale C.G., Launder B.E., editors Elsevier, New York, USA.